Asian Journal of Chemistry; Vol. 35, No. 2 (2023), 397-405

ASIAN JOURNAL OF CHEMISTRY

https://doi.org/10.14233/ajchem.2023.26935

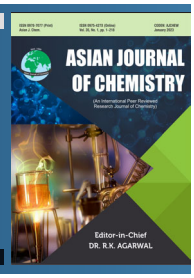

Adsorption of Chromium(VI) from Aqueous Solution using Iron Oxide Loaded Strong Base Anion Exchange Resin

HARISH N. REVANKAR[1,2], PRASANNA S. KOUJALAGI[1,2,*], VIJAYENDRA R. GURJAR[1,2] and RAVIRAJ M. KULKARNI[1,2]

[1]Department of Chemistry, K.L.S. Gogte Institute of Technology, Belagavi-590008, India
[2]Centre for Nanoscience and Nanotechnology, K.L.S. Gogte Institute of Technology (Affiliated to Visvesvaraya Technological University "Jnana Sangama" Belagavi), Belagavi-590008, India

*Corresponding author: E-mail: pskoujalagi@git.edu

Received: 16 November 2022; *Accepted*: 7 December 2022; *Published online*: 30 January 2023; AJC-21122

A hybrid adsorbent (FO-Tulsion) was prepared by altering Tulsion A-62(MP), a commercial strongly basic anion-exchanging resin, with hydrated ferric oxide (HFO) particles of average crystallite size 49.6 nm and the removal of Cr^{6+} from water on Tulsion A-62(MP) and HFO-Tulsion was observed under optimized parameters. This study examines the effectiveness of chromium(VI) removal from water utilizing Tulsion A-62(MP) and Fe-loaded Tulsion A-62(MP) as selective sorbent materials. As the resin and HFO-ion-exchange Tulsion's mechanism was rather easy and after 210 min of Cr^{6+} solution interaction, the optimum equilibrium was reached. Almost all the chromium ions was removed by the sorption process when the pH was between 4.0 and 5.0. The Freundlich and Langmuir adsorption isotherms were used to compare the equilibrium data for Cr^{6+} adsorption and it was found that both are highly suitable for Cr^{6+} adsorption. Under the same conditions, evaluation of the adsorption attainment of the prepared HFO-Tulsion and the anion resin indicated that the HFO-Tulsion had an elevated adsorption capability with a value of 207.18 mg/g than the anion resin (181.55 mg/g). The resulting hybrid resin was studied using spectroscopic and solid-state methods. Adsorption is governed by first-order reversible kinetics. It is possible that modifying anion resin with hydrated ferric oxide can greatly pick up the adsorption performance in the elimination of Cr^{6+} from drinking water and polluted water.

Keywords: Anion exchange resin, Chromium(VI), Hybrid adsorbent, Kinetics, Ferric oxide, HFO-Tulsion.

INTRODUCTION

Recently, there has been more interest in coming up with environmentally friendly ways to treat hazardous compounds in waste water, especially from urban and industrial wastewater [1-4]. Wastewaters frequently contain organic and highly toxic chemicals, such as pesticides, drugs, heavy metals, *etc*. [5-9]. Natural processes and human activities can both emit Cr(VI) into the environment [10-14]. Threats to the health of aquatic plants and wildlife were greatly increased by the heavy metal pollution of the atmosphere [15-20] and also to natural world and human beings. Because of its elevated toxicity and negative impact on human being health and the atmosphere, Cr(VI) contamination has become a major concern in many countries across the world [21-23]. Chromium(VI) compounds are more hazardous than chromium(III) compounds [24-29]. The highest permissible chromium value in drinkable water, according to WHO guidelines, is 0.05 mg/L [30-34]. Toxic Cr(VI) exposure causes cancer in the digestive system and lungs, as well as it causes nausea, vomiting, severe diarrhea, bleeding in bladder tissue [35-40].

Consequently, advanced techniques are essential for treating chromium polluted water. Several methods for removing Cr^{6+} from effluents have been proposed in the literature [41-46]. Precipitation, adsorption, phytoextraction, membrane filtration, electrodialysis and reverse osmosis are some of the techniques used. Ion exchange is the most profitable technique in conditions of simplicity, convenience, big capability and rapid rate of recovery. Ion-exchange resins provide a one-of-a-kind function in wastewater treatment. Some research has been done to use the ion-exchange approach to remove comparable ions such as vanadium [47-49]. Ion-exchange resin is a good adsorbent for removing Cr(VI) from water too. However, it showed insufficient selectivity in the presence of other competing anions

e.g. chloride, sulphate, nitrate, *etc*. which led to poor ion exchange resin adsorption efficiency. As a result, it is crucial to develop a new selective adsorbent for the removal of Cr(VI).

In recent years, ferric oxide adsorbents with polymeric bases have attracted increased interest for environmental remediation. These materials combined the advantages of polymeric ion exchange's good mechanical qualities and ferric oxide's specific affinity for the target pollutant. According to prior studies, dispersing or loading iron(III) oxide onto polymeric ion exchange can significantly increase the elimination of harmful contaminants such as chromate, arsenic, phosphate, selenium and antimony [50]. The primary purpose of this work is to evaluate Cr^{6+} adsorption capability by FO-Tulsion to that of the host Tulsion A-62 (MP). The effect of iron loading on the adsorption capacity were also evaluated.

EXPERIMENTAL

The analytical grade chemicals and reagents utilized in the analysis. Ferric chloride ($FeCl_3 \cdot 6H_2O$) was purchased from Molychem, India. The stock solution of Cr(VI) was prepared by dissolving K_2CrO_4 (Merck Life Sciences Pvt. Ltd., India) in double distilled water. Tulsion A-62(MP) is an initial ingredient for the creation of an adsorbent provided by Thermax, Ltd., India. A polystyrene-divinylbenzene matrix and positively charged quaternary ammonium functional groups make up this strong base anion exchange resin. The diameter of the resin beads ranged from 0.3 to 1.2 mm. All of the resins had already undergone pre-conditioning with 1 M NaOH and 1M HCl solutions, followed by distilled water washing and air drying. In temperature-controlled shaking unit, 30 mL of an aqueous media containing Cr^{6+} and a specified quantity of resin were stirred for 6 h at 303 K. The filtrate was tested spectrophotometrically for Cr^{6+} by a conventional diphenylcarbazide (DPC) technique at 540 nm [51]. Eqn. 1 was used to compute the Cr(VI) recovery factors [52].

$$R\ (\%) = \frac{C_a}{C_o} \times 100 \quad (1)$$

where C_a and C_o represent the amount of Cr^{6+} sorbed on the adsorptive material and during the beginning solution (mg/L), respectively.

The coefficient distribution constant (K_d) was calculated using eqn. 2:

$$K_d = \frac{q_e}{C_e} \quad (2)$$

q_e and C_e represent the concentration of metal ions (mg/L) sorbed on the adsorbent and available in the medium when it is at equilibrium.

Preparation of adsorbent (FO-Tulsion): Using the precipitation technique, hydrated iron oxide particles were loaded into the commercial strong base anion exchange resin. The preparation procedure was carried out in as reported earlier [26]. In particular, a mixture of $FeCl_3$-HCl solution with different $FeCl_3$ concentrations (0.025-3 M) was added with 5 g of Tulsion anion resin and the solutions were shaken over a range of times (2-24 h). At this point, the best conditions for preparation were investigated, which includes the optimal iron concentration determination and the time duration of reaction contact, *etc*. After filtering, the anion resins were immersed in a 1 M NaOH-NaCl solution and shaken thoroughly for 12 h at room temperature. After being rinsed with deionized water and an ethanol solution to remove any unloaded iron oxide, the solid particles were then dried at 55 ºC for 24 h. Finally, a vacuum desiccator was used to store the acquired adsorbents for further usage.

Characterization: The Nicolet iS5 FT-IR spectrometer was used to examine the surface functional groups with wave numbers ranging from 4000-400 cm^{-1}. The quantachrome NOVA 4000e instrument was utilized to estimate specific surface area and pore volumes at 77 K using the N_2 adsorption and desorption procedure. The superficial structure and components of adsorbents were investigated by a scanning electron microscope (Hitachi, model SU-1500) and energy-dispersive X-ray analysis before and after ferric oxide loading. An X-ray diffraction (XRD) analysis was used to determine the average crystallite size of Fe_2O_3 nanostructures from Scherrer's equation (eqn. 3).

$$d = \frac{k\lambda}{\beta \cos\theta} \quad (3)$$

where d = crystallites size (nm), k = 0.9 (Scherrer's constant), λ = 0.15406 nm (wavelength of X-ray source), β = full width at half maximum (FWHM) of peaks (radian), θ = peak position (radian).

RESULTS AND DISCUSSION

Adsorbents characterization: The average crystallite size of Fe_2O_3 nanostructures calculated from Scherrer's equation was found to be 49.6 nm from X-ray diffraction (XRD) analysis as shown in Fig. 1. Similarly, as shown in Fig. 2, the resin was composed of pale round yellow beads, while the modified resin (FO-Tulsion) was brown in colour. Yet, after being loaded with ferric oxide, the material retained its original spherical shape. Tulsion anion exchange resin (Fig. 3a&c) had a homogenous and flat texture, but FO-Tulsion (Fig. 3b&d) had a rough texture due to iron oxide particle accumulation. The analysis by EDX

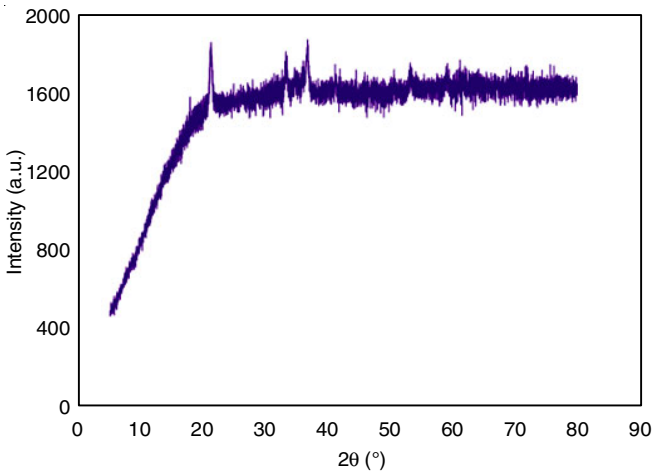

Fig. 1. X-ray diffraction of amorphous iron(III) oxide nano powder

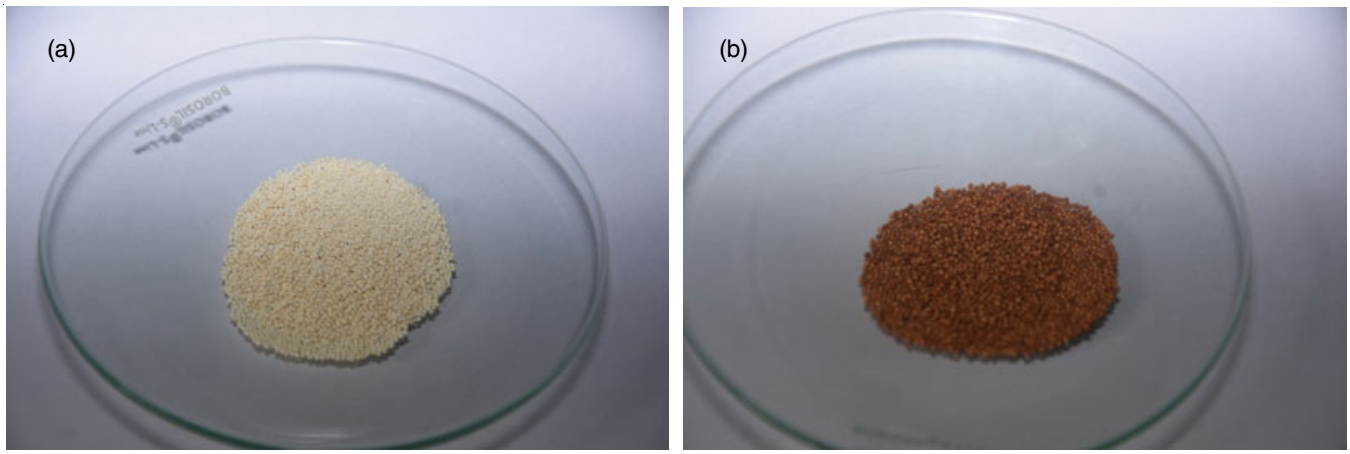

Fig. 2. Photographs of (a) Tulsion A-62(MP) (b) FO-Tulsion

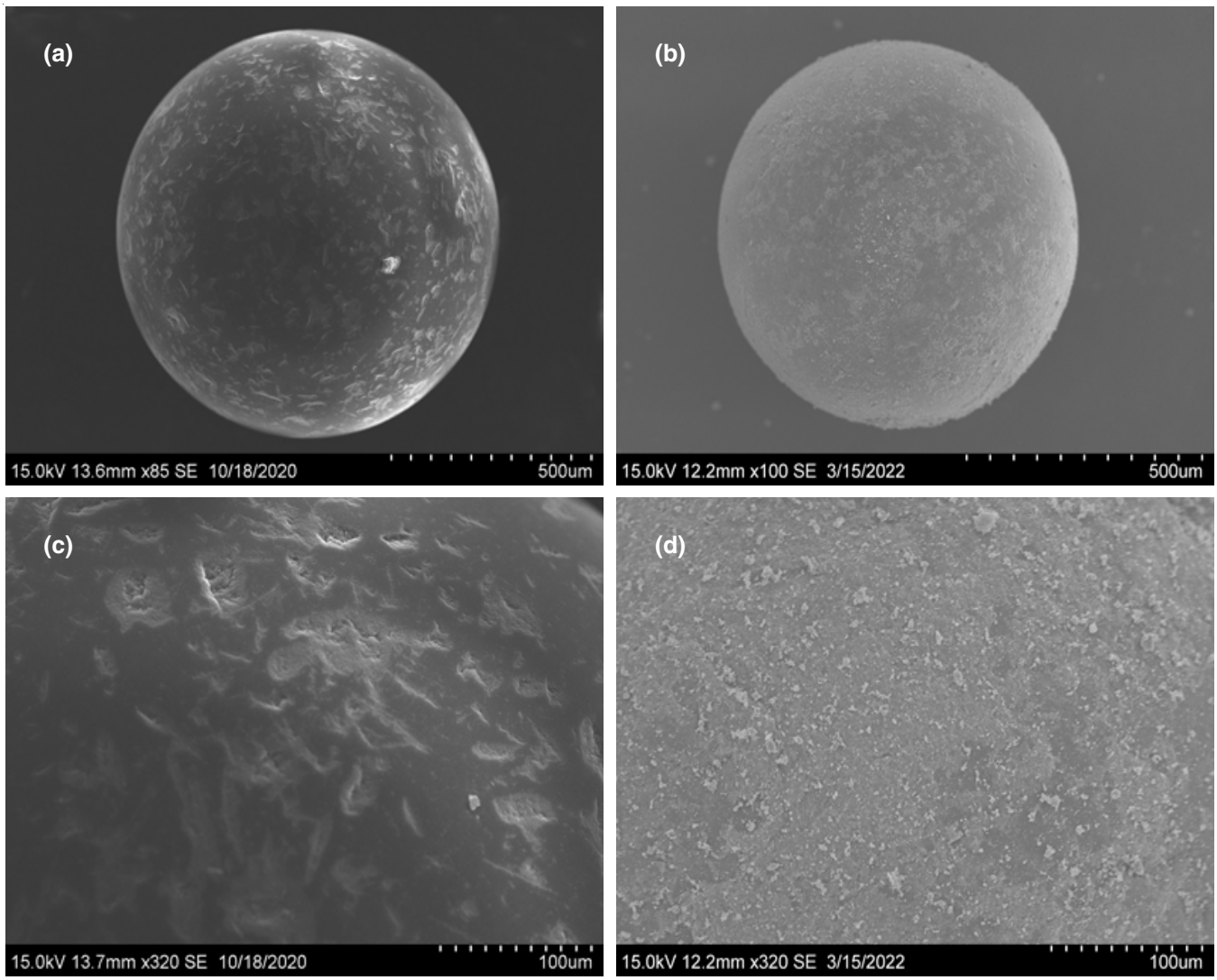

Fig. 3. SEM photographs of (a&c) Tulsion A-62(MP) and (b&d) FO-Tulsion

of anion resin and FO-Tulsion is shown in Fig. 4a-b. Tulsion A-62(MP) was found to be primarily constituted of carbon and chlorine, which might be credited to the resin's polymeric matrix and exchangeable ions. Meanwhile, the Fe element (56.92 wt.%) was identified in the FO-Tulsion elemental composition. This demonstrated that iron oxide had been successfully loaded onto the anion exchange resin.

Fig. 5 shows the spectra of FTIR of the adsorbent before and after iron oxide loading. The O-H stretching vibration of the hydroxyl group is responsible for the prominent peak at

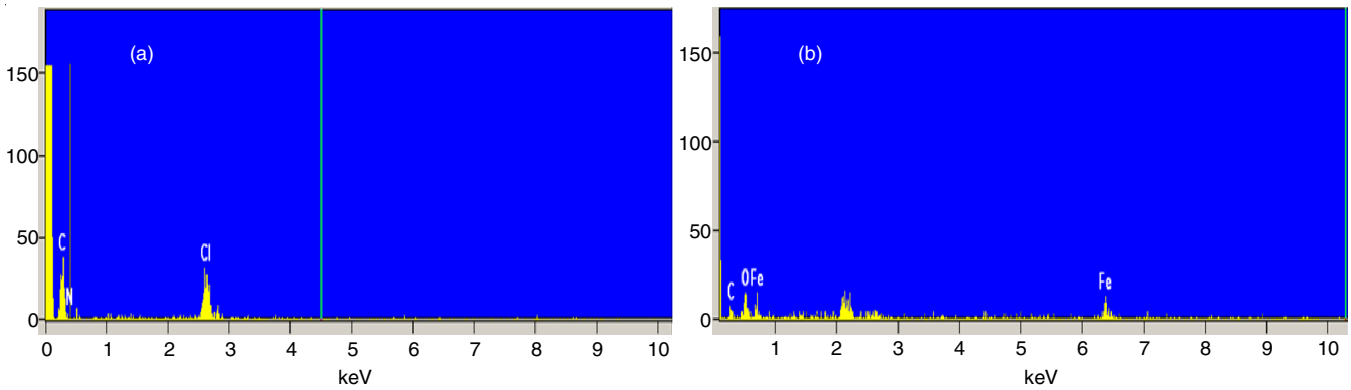

Fig. 4. EDX analysis of a) Tulsion A-62(MP) & b) FO-Tulsion

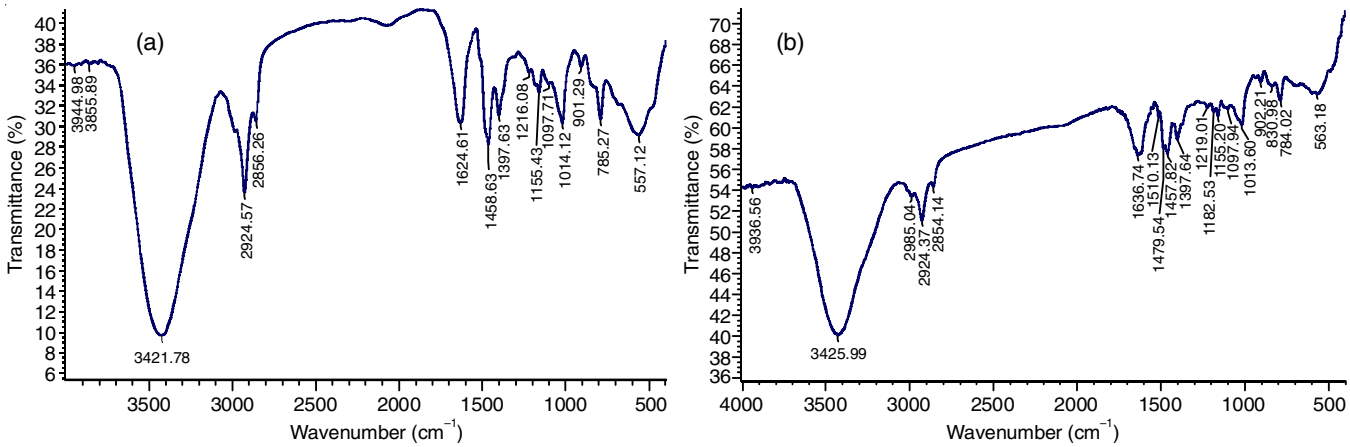

Fig. 5. FTIR spectroscopy of (a) Tulsion A-62(MP) (b) FO-Tulsion

3421 cm^{-1} in the FTIR spectra of anion exchange resin (Fig. 5a) [53,54]. The C-H stretching of the aromatic ring of polystyrene-divinylbenzene matrix in anion exchange resin is revealed by three peaks at 3015, 2924 and 2824 cm^{-1} respectively [55]. Additionally, at 1481 cm^{-1}, the quaternary ammonium functional moiety of the anion exchange resin exhibits CH_2 bending [56]. The peak patterns of the FO-Tulsion and anion exchange resin are the same, as shown in Fig. 5b. But, the presence of loaded iron oxide on anion exchange resin was clearly indicated by strong band in the vicinity of 580 cm^{-1}, which matches to the Fe-O stretching vibration [57]. Because of the excessive surface-to-mass ratio of iron oxide particles [58], the FO-Tulsion has a higher specific surface area (26.41 m^2/g) in comparison to anion exchange resin (21.84 m^2/g) (Table-1). Compared to Tulsion A-62, FO-Tulsion has a slightly reduced pore volume. These findings may be due to the loading of ferric oxide which decreases the porosity of the adsorbent and causes pore blockage.

TABLE-1
ADSORBENT'S SURFACE PROPERTIES

Adsorbents	Specific surface area by BET (m^2/g)	Pore volume (cm^3/g)
Tulsion A-62 (MP)	21.84	0.0147
FO-Tulsion	26.41	0.0135

Effect of pH: The significance of pH on the removal of chromate ions was studied using 35 mg adsorbents with 30 mL of a 213.609 mg/L chromate solution at 303 K for a predetermined period. The pH values used ranged from 3 to 9. As displayed in Fig. 6, the maximum extracting effectiveness of Cr^{6+} for Tulsion A-62(MP) and FO-Tulsion was 90% and 99%, respectively, in the 4.0 to 5.0 pH range. Adsorption was decrease at low pH levels due to contest for bonding sites between more chromate ions and hydrogen ions [59,60]. At pH levels ranging from 1 to 4, the Cr(VI) ion is mainly available in the $HCrO_4^-$ form as it is available in excess. For adsorption, the $HCrO_4^-$ ion only requires one active site on the resin phase. The presence of the non-ionic species H_2CrO_4 explains why Cr(VI) uptake is lower the elimination efficiency of Cr(VI)

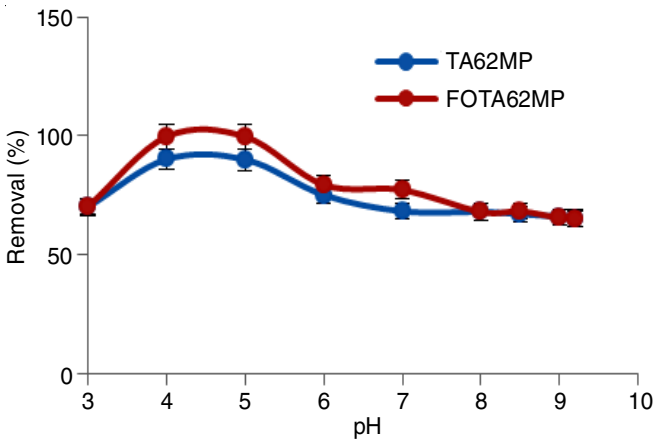

Fig. 6. pH effect on adsorption of Cr^{6+} by Tulsion A-62 (MP) & FO-Tulsion

at pH 1. At pH > 5, CrO_4^{2-} is the dominant Cr(VI) species, requiring two active sites on the resin instead of one and thus decreases after pH 5. The OH^- ions compete for the adsorption with CrO_4^{2-} ions in alkaline conditions, reducing the removal efficiency. To minimize the effects of pH change on isotherm investigations and to maintain the experimental conditions for natural water, the pH was maintained at 7.0 using bicarbonate buffer solution.

Influence of interactivity time: In batch technique, the kinetics of Cr^{6+} adsorption on Tulsion A-62(MP) & FO-Tulsion were studied using resin beads weighing 0.035 g in 30 mL of aqueous solutions with constant concentrations of Cr^{6+}. At different times, the amount of chromium(VI) that remained in the each test after adsorption was determined spectrophotometrically. According to Fig. 7, the sorption of Cr^{6+} increases as equilibration period increases and the concentration of chromium in solution decrease. Tulsion A-62(MP) & FO-Tulsion can remove about 85 & 94% of Cr^{6+} in 120 min, indicating that Cr^{6+} monolayer coverage is present on the surface of adsorbent [61]. Owing to the vast amount of accessible adsorption sites on the polymer, Cr^{6+} removal is also initially rapid. In equilibrium, increasing the contact time had little impact on Cr^{6+} adsorption due to the saturation of accessible pores on the anionic exchange resin matrix.

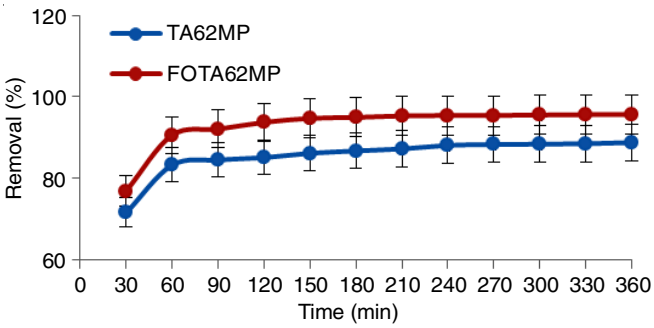

Fig. 7. Interactivity time effect on sorption of Cr^{6+} by Tulsion A-62 (MP) & FO-Tulsion

Effect of resin dosage: By aliquoting chromium solutions with a concentration of 213.6 mg/L and equilibrating them for 360 min maintaining the pH neutral with resin dosages ranging from 0.010 to 0.065 g, Tulsion A-62(MP) and FO-Tulsion equilibrium capacity were carried out. According to Fig. 8, the optimum resin dose for maximum Cr^{6+} absorption was determined to be 0.035 g after that the removal ability does not alter. Moreover some adsorption plots were left empty during the adsorption process, the removal rate increases when the adsorbent dosage is raised but reduces adsorption density [62,63]. The removal of Cr^{6+} increases with the increase in the amount of resin supply due to the availability of more accessible sites, which results in a larger surface area [64].

Impact of initial chromium(VI) concentration: In this, the effect of initial Cr^{6+} concentration affects Tulsion A-62 (MP) and FO-Tulsion for eliminating Cr^{6+}. The concentration of the synthetic soultion ranged from 149.53 to 256.33 mg/L. At 303 K, the amount of Cr^{6+} eliminated from an aqueous medium decreases as the initial concentration of Cr^{6+} increases

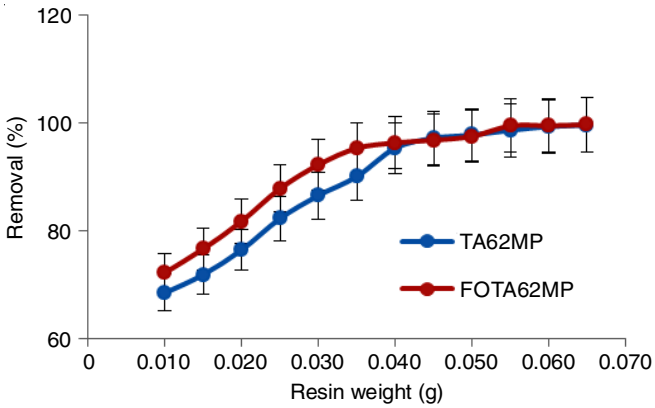

Fig. 8. Influence of resin weight on sorption of Cr^{6+} by TulsionA-62(MP) & FO-Tulsion

(Fig. 9). This is because the majority of the binding space on the ion exchange resin matrix is initially available for adsorption; however, as the strength of the Cr^{6+} ions increases, the matrix phase of the ion exchange resin becomes saturated with Cr^{6+} adsorption, and thus decreasing the elimination of Cr^{6+} ions.

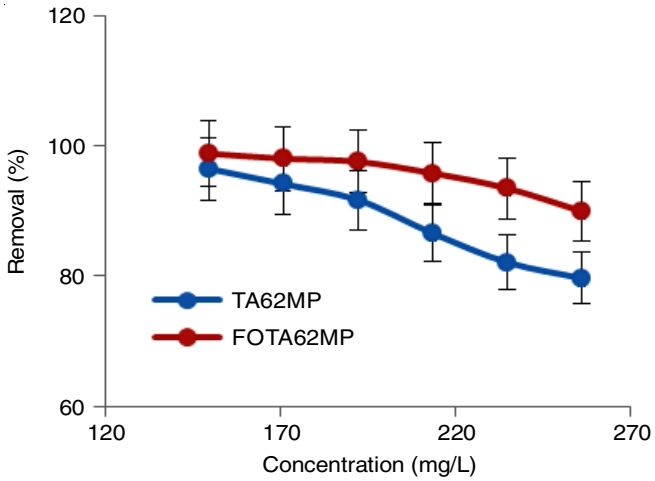

Fig. 9. Impact of initial concentration for removal of Cr^{6+} by TulsionA-62(MP) & FO-Tulsion

Isotherm models: To illustrate the adsorption behaviour of metals by various adsorbents, three well-known isotherm models *viz.* Langmuir, Freundlich and Redlich-Peterson isotherms were applied [65,66].

Langmuir isotherm model is represented as:

$$\frac{C_e}{q_e} = \left(\frac{1}{K_L q_m}\right) + \frac{C_e}{q_m} \quad (4)$$

where, the constants C_e and q_e denote the concentrations of metal ions in the initial and equilibrium environments and q_m and K_L, respectively, stand for the ion exchange capacity and adsorption energy.

A linear curve in Fig. 10 illustrates the Langmuir isotherm following adsorption on Tulsion A-62 and FO-Tulsion. This isotherm states that the homogenous monolayer adsorption on the adsorbent surface has same activation energy. According to the Langmuir isotherm, the maximal adsorption capacities

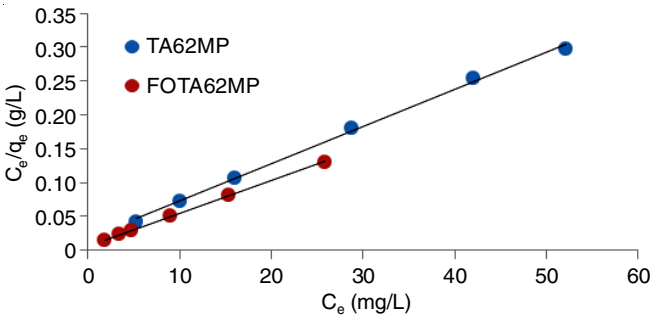

Fig. 10. Langmuir isotherm for Cr^{6+} sorption on Tulsion A-62(MP) & FO-Tulsion

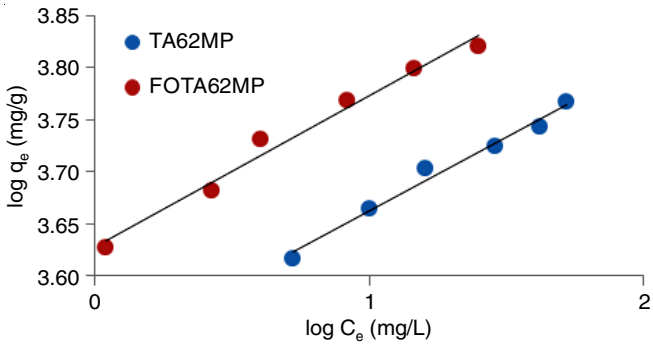

Fig. 11. Freundlich isotherm for Cr^{6+} sorption on Tulsion A-62(MP) & FO-Tulsion

(q_m) of FO-Tulsion and anion exchange resin were 207.2 and 181.5 mg/g, respectively. The increased surface area caused by the presence of iron(III) oxide was attributed to the higher adsorption capacity of FO-Tulsion, which offered more adsorption sites on the adsorbent surface for Cr(VI) adsorption [65]. Furthermore, the formation of an inner sphere complex between ferric oxide and Cr(VI) will boost adsorption affinity [66]. Also, the addition of Fe may increase the positive charges on the adsorbent surface, resulting in the greater electrostatic interaction between chromate and iron oxide [66]. As a result, it can be concluded that iron oxide loading is an essential element in increasing the adsorption capacity of anion exchange resin [67]. Moreover, the values of parameter "n" obtained in this investigation were greater than unity for both adsorbents (Table-2), indicating that Cr(VI) adsorption was favourable on both FO-Tulsion and strong base anion exchange resin.

A linear equation called the Freundlich adsorption isotherm model depicts a system with heterogeneous surface energy (eqn. 5).

$$\log q_e = \log K_F + \frac{1}{n}\log C_e \quad (5)$$

where C_e is the concentration of metal ions at equilibrium and q_e is the adsorption capacity at equilibrium. The constants K_F and n are obtained from the log q_e *vs.* log C_e plot (Fig. 11). The adsorption capability of Tulsion A-62 and FO-Tulsion increases as K_F increases. According to Table-2, the equilibrium parameters followed Langmuir, Freundlich and Redlich-Peterson models. Because of ($0 < R_L < 1$), the sorption of Cr^{6+} on Tulsion A-62 and FO-Tulsion is favourable [67].

The adsorption process is also heterogeneous and does not adhere to ideal monolayer adsorption since the Redlich-Peterson isotherm is a mixture of the Freundlich-Langmuir isotherm. The linear form of the Redlich-Peterson equation is represented as:

$$\ln\frac{C_e}{q_e} = \beta \ln C_e - \ln A \quad (6)$$

where A (L/g) is the Redlich-Peterson isotherm's constant factor and the exponent is a value between 0 and 1.

Kinetics of Cr^{6+} adsorption: Reversible first-order kinetics was used to characterize the rate of Cr^{6+} ions sorption on the Tulsion A-62 and FO-Tulsion. It also suggests a retention time for metal ions on Tulsion A-62 and FO-Tulsion. For Cr^{6+} adsorption from aqueous media at 213.6 mg/L concentration, the forward (k_f), backward (k_b) and rate of reaction coefficients (k) [68,69] were calculated. Table-3 shows that for both types of adsorbents, the forward rate constant for removing Cr^{6+} is significantly higher than the backward rate constant. This proved that the rate of adsorption is the dominant factor.

Thermodynamics studies: Applying the conventional thermodynamic equations, the effect of temperature on Cr^{6+} adsorption by Tulsion A-62(MP) and FO-Tulsion was used to calculate the quantifiable thermodynamic factors, such as the change in Gibbs free energy (ΔG), change in enthalpy (ΔH) and change in entropy (ΔS) [70,71]:

$$\ln K_d = \frac{\Delta S}{R} - \frac{\Delta H}{RT} \quad (7)$$

TABLE-2
PARAMETERS OF ADSORPTION ISOTHERMS

Resin	Freundlich isotherm			Langmuir isotherm				Redlich-Peterson isotherm		
	K_F (L/mg)	n	R^2	K_L (L/g)	A_s (mg/g)	R^2	R_L	β	A (L/g)	R^2
Tulsion A-62(MP)	3311.2	7.03	0.981	0.31	181.5	0.997	0.0160	0.858	0.116	0.999
FO - Tulsion	3951.8	5.98	0.965	0.71	207.2	0.999	0.0071	0.833	0.138	0.998

TABLE-3
RATE CONSTANTS OF Cr^{6+} IONS REMOVAL FROM AQUEOUS SOLUTION BY ADSORBENTS

Adsorbent	Cr^{6+} concentration (mg/L)	Overall rate constant, $k = k_1 + k_2$ (min^{-1})	Forward rate constant, k_1 (min^{-1})	Backward rate constant, k_2 (min^{-1})
Tulsion A-62(MP)	213.6	0.0121	0.0108	0.00134
FO-Tulsion	213.6	0.0197	0.0188	0.00090

TABLE-4
PARAMETERS OF THERMODYNAMICS FOR Cr^{6+} SORPTION BY ADSORBENTS

Adsorbents	Temp. (K)	log K_d	ΔG (kJ mol^{-1})	ΔH (kJ mol^{-1})	ΔS (kJ mol^{-1} K^{-1})
Tulsion A-62(MP)	303	0.9597	-2.42	0.10	0.010
	313	0.9613	-2.50		
	323	0.9622	-2.58		
FO-Tulsion	303	1.4466	-3.64	7.75	0.038
	313	1.5771	-4.10		
	323	1.6365	-4.39		

$$\Delta G = \Delta H - T\Delta S \quad (8)$$

$$K_d = \frac{C_s}{C_e} \quad (9)$$

C_e stands for the equilibrium concentration of Cr^{6+} in aqueous media (mg/L), C_s for the equilibrium concentration of adsorbed Cr^{6+} on the resin surface (mg/L), R for the ideal gas constant (8.314 J/mol K) and T for the kelvin temperature. K_d stands for the adsorption equilibrium constant. Enthalpy and entropy change values were calculated using the slope and intercept of ln K_d *vs.* 1/T plots. Table-4 displays the thermodynamic parameters for Tulsion A-62(MP) and FO-Tulsion. The negative values of ΔG values indicated that adsorption occurs spontaneously, while the endothermic character of the adsorption process was demonstrated by the positive ΔH values, with higher temperatures being more acceptable. The positive ΔS values indicated that the adsorption process at the solid/liquid interface is unpredictable.

Desorption studies: Adsorbents should typically be regenerated for reuse because the adsorption efficiency typically does not give enough information for an adsorbent to be employed in a practical applications. In desorption studies, the prepared base anion exchange resin was utilized in order to reuse resin. During the course of 6 h, 30 mL of Cr(VI) solution with a concentration of 213.609 mg/L was in contact with 35 mg of resin in a temperature-controlled water bath shaker operating at 303 K. After Cr(VI) has been adsorbed onto the resin, the resin was washed with de-ionized water to get rid of any remaining solution. The cleaned resin was treated with 30 mL of desorbents, including 0.4% NaOH for host strong base anion exchange resin and a binary solution of 5% NaOH and 5% NaCl (pH = 12.5) used for hybrid resin FOTA62MP and then shaken for 6 h. The concentration of Cr(VI) in the filtrate was assessed using desorption eqn. 10. The recovery of Cr(VI) from TA62MP and FOTA62MP was 94.7% and 91.4%, respectively, in the first cycle. The recovery of Cr(VI) from TA62MP and FOTA62MP was 85.0% and 84.5%, respectively, in the fifth cycle (Fig. 12). The difference in Cr(VI) recovery between TA62MP and FOTA62MP may be due to weak non-specific ion exchange or electrostatic attraction of Cr(VI) onto Tulsion A-62(MP) as compared to FO-Tulsion particular affinity toward chromate *via* ligand exchange with the hydroxyl groups (strong interaction).

$$\text{Desorption ratio} = \frac{\text{Amount of metal ion desorbed}}{\text{Amount of metal ion adsorbed}} \times 100 \quad (10)$$

Conclusion

In this work, two hybrid ion-exchange resins Tulsion A-62(MP) and Fe-loaded Tulsion A-62(MP) were found to be effective adsorbents towards the removal of Cr^{6+} ions when the pH was between 4.0 and 5.0. The amount of resin used and the chromium content determine the kinetics of Cr^{6+} adsorption. As agitation time increased, Cr^{6+} adsorption increased and achieved the equilibrium at 210 min. The separation factor R_L value between 0 and 1 favours the Cr^{6+} adsorption. Under optimal conditions, the FO-Tulsion has a significantly higher adsorption capacity than Tulsion A-62(MP). The equilibrium adsorption data for both FO-Tulsion and Tulsion A-62(MP) were well matched by the Langmuir, Freundlich and Redlich-Peterson isotherm models. The results showed that FO-Tulsion is a potential adsorbent for chromium(VI) removal from the aqueous solutions.

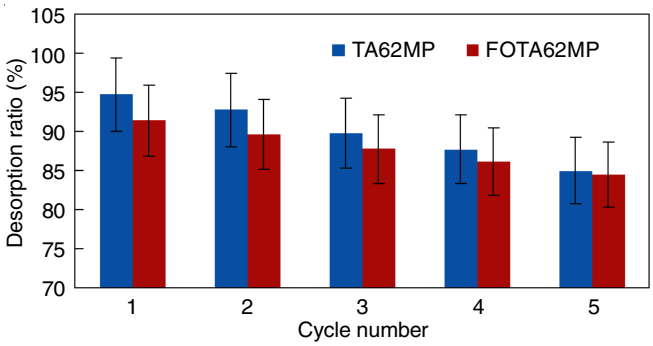

Fig. 12. Cr^{6+} Desorption ratios of Tulsion A-62 & FO-Tulsion

ACKNOWLEDGEMENTS

The authors gratefully acknowledge Thermax Limited, Pune, India, for providing the ion exchanger used in this study.

CONFLICT OF INTEREST

The authors declare that there is no conflict of interests regarding the publication of this article.

REFERENCES

1. A.K. Goyal, E.S. Johal and G. Rath, *Curr. Nanosci.*, **7**, 640 (2011); https://doi.org/10.2174/157341311796196772
2. P. Meshram, A. Ghosh, Y. Ramamurthy and B.D. Pandey, *Russ. J. Non-Ferrous Met.*, **59**, 533 (2018); https://doi.org/10.3103/S1067821218050103
3. J.A.S. Tenorio and D.C.R. Espinosa, *Waste Manag.*, **21**, 637 (2001); https://doi.org/10.1016/S0956-053X(00)00118-5
4. Y. Xie, J. Lin, H. Lin, Y. Jiang, J. Liang, H. Wang, S. Tu and J. Li, *J. Hazard. Mater.*, **392**, 122496 (2020); https://doi.org/10.1016/j.jhazmat.2020.122496
5. A. Sowmya and S. Meenakshi, *Desalination Water Treat.*, **51**, 7145 (2013); https://doi.org/10.1080/19443994.2013.771286

6. A. Gautam, A. Kushwaha and R. Rani, *Curr. Microbiol.*, **79**, 33 (2021); https://doi.org/10.1007/s00284-021-02734-z
7. G. Sarojini, S. Venkatesh Babu, N. Rajamohan, P. Senthil Kumar and M. Rajasimman, *Environ. Res.*, **201**, 111626 (2021); https://doi.org/10.1016/j.envres.2021.111626
8. S.M. Matome, E. Makhado, L.M. Katata-Seru, T.C. Maponya, K.D. Modibane, M.J. Hato and I. Bahadur, *S. Afr. J. Chem. Eng.*, **34**, 1 (2020); https://doi.org/10.1016/j.sajce.2020.05.004
9. S. Rapti, A. Pournara, D. Sarma, I.T. Papadas, G.S. Armatas, A.C. Tsipis, T. Lazarides, M.G. Kanatzidis and M.J. Manos, *Chem. Sci.*, **7**, 2427 (2016); https://doi.org/10.1039/C5SC03732H
10. N. Ballav, A. Maity and S.B. Mishra, *Chem. Eng. J.*, **198-199**, 536 (2012); https://doi.org/10.1016/j.cej.2012.05.110
11. E.M. Hamilton, S.D. Young, E.H. Bailey and M.J. Watts, *Food Chem.*, **250**, 105 (2018); https://doi.org/10.1016/j.foodchem.2018.01.016
12. W. Liu, L. Yang, S. Xu, Y. Chen, B. Liu, Z. Li and C. Jiang, *RSC Adv.*, **8**, 15087 (2018); https://doi.org/10.1039/C8RA01805G
13. R. Jayakumar, M. Rajasimman and C. Karthikeyan, *J. Environ. Chem. Eng.*, **2**, 1261 (2014); https://doi.org/10.1016/j.jece.2014.05.007
14. B. Choudhary and D. Paul, *J. Environ. Chem. Eng.*, **6**, 2335 (2018); https://doi.org/10.1016/j.jece.2018.03.028
15. H. Deveci and Y. Kar, *J. Ind. Eng. Chem.*, **19**, 190 (2013); https://doi.org/10.1016/j.jiec.2012.08.001
16. F.O. Ntuli and V.E. Pakade, *Chem. Eng. Commun.*, **207**, 279 (2020); https://doi.org/10.1080/00986445.2019.1581619
17. R.F.S. Barbosa, A.G. Souza, H.F. Maltez and D.S. Rosa, *Chem. Eng. J.*, **395**, 125055 (2020); https://doi.org/10.1016/j.cej.2020.125055
18. N. Sharma, K.K. Sodhi, M. Kumar and D.K. Singh, *Environ. Nanotechnol. Monit. Manag.*, **15**, 100388 (2021); https://doi.org/10.1016/j.enmm.2020.100388
19. F. Fu, J. Ma, L. Xie, B. Tang, W. Han and S. Lin, *J. Environ. Manage.*, **128**, 822 (2013); https://doi.org/10.1016/j.jenvman.2013.06.044
20. H. Dong, J. Deng, Y. Xie, C. Zhang, Z. Jiang, Y. Cheng, K. Hou and G. Zeng, *J. Hazard. Mater.*, **332**, 79 (2017); https://doi.org/10.1016/j.jhazmat.2017.03.002
21. S. Zhu, X. Huang, D. Wang, L. Wang and F. Ma, *Chemosphere*, **207**, 50 (2018); https://doi.org/10.1016/j.chemosphere.2018.05.046
22. Y. Wang, D. Zhao, S. Feng, Y. Chen and R. Xie, *J. Colloid Interface Sci.*, **580**, 345 (2020); https://doi.org/10.1016/j.jcis.2020.07.016
23. W. Zhang, L. Qian, D. Ouyang, Y. Chen, L. Han and M. Chen, *Chemosphere*, **221**, 683 (2019); https://doi.org/10.1016/j.chemosphere.2019.01.070
24. Y. Guo, X. Wei, K. Zhang, J. Zhang, L. Mi, Z. Wu, G. Wang, Y. Li, Q. Huang, W. Fu, Y. Zhang, A. Hou, H. Wang and X. Qi, *J. Dispers. Sci. Technol.*, (2020); https://doi.org/10.1080/01932691.2020.1842761
25. W. Jianlong, Z. Xinmin and Q. Yi, *J. Environ. Sci. Health Part A Tox. Hazard. Subst. Environ. Eng.*, **35**, 1211 (2000); https://doi.org/10.1080/10934520009377029
26. M.R. Boldaji, R. Nabizadeh, M.H. Dehghani, K. Nadafi and A.H. Mahvi, *J. Environ. Sci. Health Part A Tox. Hazard. Subst. Environ. Eng.*, **45**, 946 (2010); https://doi.org/10.1080/10934521003772337
27. G. Al-Enezi, M.F. Hamoda and N. Fawzi, *J. Environ. Sci. Health Part A Tox. Hazard. Subst. Environ. Eng.*, **39**, 455 (2004); https://doi.org/10.1081/ESE-120027536
28. S. Verbych, N. Hilal, G. Sorokin and M. Leaper, *Sep. Sci. Technol.*, **39**, 2031 (2005); https://doi.org/10.1081/SS-120039317
29. F. Gorzin and M. Bahri Rasht Abadi, *Adsorpt. Sci. Technol.*, **36**, 149 (2018); https://doi.org/10.1177/0263617416686976
30. Y. Zhang, G. Lan, Y. Liu, T. Zhang, H. Qiu, F. Li, J. Yan and Y. Lu, *Sep. Sci. Technol.*, **56**, 2532 (2021); https://doi.org/10.1080/01496395.2020.1842451
31. M. Nigam, S. Rajoriya, S. Rani Singh and P. Kumar, *J. Environ. Chem. Eng.*, **7**, 103188 (2019); https://doi.org/10.1016/j.jece.2019.103188
32. L. Li, Y. Li, Y. Liu, L. Ding, X. Jin, H. Lian and J. Zheng, *Water*, **13**, 3602 (2021); https://doi.org/10.3390/w13243602
33. A. Murugesan, T. Vidhyadevi, S.D. Kirupha, L. Ravikumar and S. Sivanesan, *Environ. Prog. Sustain. Energy*, **32**, 673 (2013); https://doi.org/10.1002/ep.11684
34. M. Ghashghaee and V. Farzaneh, *Iran. J. Toxicol.*, **10**, 15 (2016).
35. M.A. Islam, M.J. Angove and D.W. Morton, *Environ. Nanotechnol. Monit. Manag.*, **12**, 100267 (2019); https://doi.org/10.1016/j.enmm.2019.100267
36. S. Edebali and E. Pehlivan, *Chem. Eng. J.*, **161**, 161 (2010); https://doi.org/10.1016/j.cej.2010.04.059
37. P.S. Koujalagi, S.V. Divekar, R.M. Kulkarni and R.K. Nagarale, *Desalination Water Treat.*, **51**, 3273 (2013); https://doi.org/10.1080/19443994.2012.749049
38. S.S. Salih and T.K. Ghosh, *Cogent Environ. Sci.*, **3**, 1401577 (2017); https://doi.org/10.1080/23311843.2017.1401577
39. F. Fu and Q. Wang, *J. Environ. Manage.*, **92**, 407 (2011); https://doi.org/10.1016/j.jenvman.2010.11.011
40. D. Petruzzelli, R. Passino and G. Tiravanti, *Ind. Eng. Chem. Res.*, **34**, 2612 (1995); https://doi.org/10.1021/ie00047a009
41. X. Li, S. Shi, H. Cao, Y. Li and D. Xu, *Russ. J. Phys. Chem. A. Focus Chem.*, **92**, 1229 (2018); https://doi.org/10.1134/S0036024418060237
42. S.S. Baral, S.N. Das, P. Rath, G. Roy Chaudhury and Y.V. Swamy, *Chem. Ecol.*, **23**, 105 (2007); https://doi.org/10.1080/02757540701197697
43. V. Kumar and S.K. Dwivedi, *J. Clean. Prod.*, **295**, 126229 (2021); https://doi.org/10.1016/j.jclepro.2021.126229
44. B. Rzig, F. Guesmi, M. Sillanpää and B. Hamrouni, *Water Sci. Technol.*, **84**, 552 (2021); https://doi.org/10.2166/wst.2021.233
45. H.C. Yalcin and A. Kaushik, *Emergent Mater.*, **4**, 1 (2021); https://doi.org/10.1007/s42247-021-00189-3
46. Z.A. Al-Jaser and M.F. Hamoda, *Desalination Water Treat.*, **157**, 148 (2019); https://doi.org/10.5004/dwt.2019.24127
47. D. Kauspediene, E. Kazlauskiene, R. Cesuniene, A. Gefeniene, R. Ragauskas and A. Selskiene, *Chemija*, **24**, 171 (2013).
48. S. Ghosh, K.J. Dhole, M.K. Tripathy, R. Kumar and R.S. Sharma, *J. Radioanal. Nucl. Chem.*, **304**, 917 (2015); https://doi.org/10.1007/s10967-014-3906-3
49. S.M. Alshehri, M. Naushad, T. Ahamad, Z.A. Alothman and A. Aldalbahi, *Chem. Eng. J.*, **254**, 181 (2014); https://doi.org/10.1016/j.cej.2014.05.100
50. K.A. Gebru and C. Das, *Chemosphere*, **191**, 673 (2018); https://doi.org/10.1016/j.chemosphere.2017.10.107
51. D. Li, H. Song, X. Meng, T. Shen, J. Sun, W. Han and X. Wang, *Nanomaterials*, **10**, 546 (2020); https://doi.org/10.3390/nano10030546
52. E. Álvarez-Ayuso, *Water Res.*, **37**, 4855 (2003); https://doi.org/10.1016/j.watres.2003.08.009
53. J. Elton, K. Hristovski and P. Westerhoff, *ACS Symp. Ser.*, **1123**, 223 (2013); https://doi.org/10.1021/bk-2013-1123.ch013
54. P.S. Koujalagi, S.V. Divekar and R.M. Kulkarni, *Asian J. Chem.*, **30**, 1083 (2018); https://doi.org/10.14233/ajchem.2018.21188
55. M.A. Hanif, R. Nadeem, H.N. Bhatti, N.R. Ahmad and T.M. Ansari, *J. Hazard. Mater.*, **139**, 345 (2007); https://doi.org/10.1016/j.jhazmat.2006.06.040
56. S. Rengaraj, K.H. Yeon, S.Y. Kang, J.U. Lee, K.W. Kim and S.H. Moon, *J. Hazard. Mater.*, **92**, 185 (2002); https://doi.org/10.1016/S0304-3894(02)00018-3

57. S. Rengaraj and S.H. Moon, *Water Res.*, **36**, 1783 (2002); https://doi.org/10.1016/S0043-1354(01)00380-3
58. J. Al-Abdullah, A.G. Al Lafi, T. Alnama, W. Al Masri, Y. Amin and M.N. Alkfri, *Iran. J. Chem. Chem. Eng.*, **37**, 131 (2018).
59. Q. Yu and P. Kaewsarn, *Sep. Sci. Technol.*, **34**, 1595 (1999); https://doi.org/10.1080/01496399909353759
60. B. Haerizade, M. Ghavami and M. Koohi, *Iran. J. Chem. Chem. Eng.*, **37**, 29 (2018).
61. M. Kondalkar, U. Fegade, Inamuddin, S. Kanchi, T. Altalhi, K.E. Suryawanshi and A.M. Patil, *J. Phys. Chem. Solids*, **163**, 110544 (2022); https://doi.org/10.1016/j.jpcs.2021.110544
62. D. Haddad, A. Mellah, D. Nibou and S. Khemaissia, *J. Environ. Eng.*, **144**, 04018027 (2018); https://doi.org/10.1061/(ASCE)EE.1943-7870.0001349
63. F. Gode and E.A. Pehlivan, *J. Hazard. Mater.*, **100**, 231 (2003); https://doi.org/10.1016/S0304-3894(03)00110-9
64. T. Cheng, C. Chen, R. Tang, C. Han and Y. Tian, *Iran. J. Chem. Chem. Eng.*, **37**, 61 (2018).
65. T. Shi, Z. Wang, Y. Liu, S. Jia and D. Changming, *J. Hazard. Mater.*, **161**, 900 (2009); https://doi.org/10.1016/j.jhazmat.2008.04.041
66. B. Singha and S.K. Das, *Colloids Surf. B Biointerfaces*, **84**, 221 (2011); https://doi.org/10.1016/j.colsurfb.2011.01.004
67. P.S. Koujalagi, S.V. Divekar, R.M. Kulkarni and E.M. Cuerda-Correa, *Desalination Water Treat.*, **57**, 23965 (2016); https://doi.org/10.1080/19443994.2016.1138329
68. D. Goyal and A. Mishra, *Curr. Environ. Eng.*, **1**, 191 (2015); https://doi.org/10.2174/2212717801031505221632 48
69. E.C.M. de Moura, P.R. do Vale Souza Gois, D.R. da Silva, D.M. de Araujo and C.A. Martinez-Huitle, *Curr. Anal. Chem.*, **13**, 202 (2017); https://doi.org/10.2174/1573411012666160622081420
70. T. Metidji, H. Bendjeffal, A. Djebli, H. Mamine, H. Bekakria and Y. Bouhedja, *Recent Innov. Chem. Eng.*, **14**, 259 (2021); https://doi.org/10.2174/2405520414666210203221527
71. S. Parlayici, K.T. Sezer and E. Pehlivan, *Curr. Anal. Chem.*, **16**, 880 (2020); https://doi.org/10.2174/1573411015666191114143128
72. F. Shahram Forouz, S.A. Hosseini Ravandi and A.R. Allafchian, *Curr. Nanosci.*, **12**, 266 (2016); https://doi.org/10.2174/1573413712999151216162920